NANOPARTICLE LOADED FAST-DISSOLVING MICRONEEDLE PATCH FOR LOCAL DELIVERY OF ANESTHETIC AGENT – DUAL-ACTION APPROACH

DAHAI QIU,[*] YAO LI,[*] JUN XU[*] and ZULCAIF AHMAD[**]

[*]*Department of Surgical Anesthesiology, Central Hospital affiliated to Shandong First Medical University, Jinan 250000, China*
[**]*Department of Pharmacy, University of Rasul, Mandi Bahauddin 50380, Pakistan*
✉ *Corresponding author: J. Xu, junxu_584521@126.com*

Received July 2, 2025

This study aimed to develop a dual-action fast-dissolving microneedle patch (FDMN) through which lidocaine could be delivered transdermally and to obtain a combined effect with free drug for rapid onset and nanoparticles for sustained release. First, chitosan-based nanoparticles were tried, but found incompatible with HA-PVP microneedle matrix, then HPMC-based nanoparticles were prepared and proceeded. The average particle size of nanoparticles was 71.4 ± 2.28 nm with PDI of 0.312. Zeta potential was -0.1 mV. Drug entrapment and loading efficiencies were found to be 94.5 ± 1.93% and 8.5 ± 0.65%, respectively. The FDMN6 patch had suitable morphology, consistent thickness (0.173 ± 0.01 mm) and mechanical strength. *Ex-vivo* studies showed 92.87 ± 0.88% lidocaine release over 480 minutes, following first-order kinetics ($R^2 = 0.983$). The patch was biocompatible and *in-vivo* testing confirmed a rapid onset and prolonged anesthetic effect up to 480 minutes. The dual-action FDMN6 patch provides a pain-free alternative for localized anesthesia. It offers immediate and sustained delivery of lidocaine. Its safety, ease of application and extended efficacy highlighted its potential for minor surgical procedures.

Keywords: anesthesia, microneedles, nanoparticles, transdermal drug delivery system, lidocaine

INTRODUCTION

Localized anesthetic agents are very important in the management of pain during a surgical or dermatological procedure.[1,2] Lidocaine is an example of a local anesthetic and a popular one among amides, which has a rapid onset and moderate duration of action. However, its topical delivery from creams, gels and injections has several limitations such as poor skin permeability, short duration of anesthesia, inconsistent skin penetration, poor patient compliance due to fear of injection pain, feeling of discomfort at the injection site and possible systemic toxicity.[3,4] Some other innovative techniques have to be used to make drug delivery more effective and patient-friendly.

Microneedle (MN) patches have shown a promising approach for a transdermal drug delivery system that painlessly gets in through the stratum corneum and improves delivery of the drug.[5-8] Fast-dissolving microneedle (FDMN) patches developed with biocompatible polymer materials have much better characteristics, like fast dissolution, simple application, and controlled drug delivery.[9] The existing lidocaine microneedle patches, unfortunately, provide a single-phase immediate drug release.

Biodegradable polymers are critical in fabricating microneedle patches regarding appropriate mechanical strength, drug loading, and controlled release.[10] Chitosan and hydroxypropyl methylcellulose (HPMC) are naturally derived polysaccharides used widely for nanoparticle preparation due to their biocompatible nature, mucoadhesive characteristics, and ability to stabilize drugs.[11-13] On the other hand, hyaluronic acid (HA), being hydrophilic, will cause rapid dissolution of the microneedle upon piercing the skin, while providing hydration and tissue compatibility.[14-16] Polyvinylpyrrolidone (PVP) is a synthetic polymer with excellent film formation properties and gives mechanical strength to the microneedle structure, while allowing quick disintegration for efficient drug release.[17-19]

Therefore, the different combinations of these polymers represent a good platform for transdermal drug delivery, having a balance of structural integrity and dissolution kinetics.[20-25]

To overcome this gap, a fast-dissolving microneedle patch that contains both free lidocaine for quick analgesic effects and HPMC-based lidocaine nanoparticles for continuous release is proposed. This method seeks to increase anesthesia duration, while rapidly relieving pain, potentially enhancing patient adherence and maximizing procedural efficiency. The formulation of these microneedles includes HA and PVP to ensure strength and fast dissolution, while the HPMC nanoparticles improve drug stability and prolong retention at the site of administration.[26]

This research was focused on the development, characterization, and evaluation of a novel dual-release lidocaine microneedle patch. The developed FDMN patch was evaluated in terms of average particle size (zeta sizer), zeta potential, structural integrity and uniformity (optical microscopy), uniformity of thickness, surface morphology (scanning electron microscopy), functional groups (Fourier transform infrared spectroscopy), drug loading efficiency, insertion of microneedles, *ex-vivo* release, biocompatibility testing (irritation study), and its *in-vivo* anesthetic efficacy to establish its potential as an advanced transdermal anesthetic platform. This study hypothesized that a dual-action microneedle patch could achieve both rapid onset and sustained anesthesia.

EXPERIMENTAL

Materials

Chitosan HMW (~70000-90000), hydroxyl propyl methylcellulose (HPMC) and polyvinyl pyrrolidone K30 were purchased from Sigma Aldrich, Germany. Hyaluronic acid and citric acid were gifted by Unison Pharmaceuticals, Pakistan. Lidocaine was gifted by Ameer Adnan Pharmaceuticals, Pakistan. A silicon microneedle mold (ST-12, 15 X 15, height 500 µm and base = 200 µm) was purchased from Micropoint Technology, Singapore.

Methods

Preparation of nanoparticle loaded fast-dissolving microneedle patch

Preparation of lidocaine nanoparticles

Lidocaine-loaded nanoparticles were prepared by using an ionic gelation method with chitosan and HPMC. Citric acid was utilized as crosslinking agent.[27,28] Firstly, different concentrations of polymeric solution were prepared separately (Table 1) at room temperature under continued stirring on the magnetic stirrer for 2 hours for complete dissolution. For chitosan, 1% (v/v) acetic acid solution was used as a solvent and HPMC was dissolved in distilled water. A 2% lidocaine solution was prepared in ethanol and poured into the polymeric solution and stirred for 30 minutes. Next, an aqueous solution of 0.1% citric acid was prepared and added dropwise to the polymeric-lidocaine mixture under magnetic stirring (1000 rpm) to promote nanoparticle formation via ionic gelation. The suspension was stirred for another 2 hours to ensure complete crosslinking. Nanoparticles were isolated by centrifugation at 12000 rpm for 30 minutes at 4 °C and washed three times with deionized water to eliminate unreacted materials. The purified nanoparticles were then lyophilized and stored at 4 °C until further study.

Fabrication of hyaluronic acid and PVP-based fast-dissolving microneedles

The FDMNs patches were prepared by using the solvent-casting method[29] with a two-stage formulation approach. In the first stage, the homogeneous polymeric solution was prepared with different concentrations of HA and PVP in deionized water under continuous stirring at room temperature. Moreover, polyethylene glycol 400 (PEG) was also added in some formulations, as shown in Table 1.

Table 1
Composition of nanoparticle-loaded FDMN patches

Formulation	Chitosan, % (w/v)	HPMC, % (w/v)	Hyaluronic acid, % (w/v)	PVP, % (w/v)	PEG, % (v/v)
FDMN1	0.5	-	0.5	2.5	-
FDMN2	0.5	-	1.0	5.0	-
FDMN3	-	1.0	0.5	2.5	-
FDMN4	-	1.5	0.5	5.0	-
FDMN5	-	1.0	1.0	2.5	1.0
FDMN6	-	1.5	1.0	5.0	1.0

The mixture was stirred for 1 hour to achieve a uniform dispersion. Next, 2% (w/v) lidocaine was dissolved in ethanol and then added dropwise and mixed into the HA-PVP solution until a homogeneous mix was achieved. This solution is referred to as Solution A. In the second stage, previously synthesized polymeric-

lidocaine nanoparticles were then suspended in Solution A with gentle stirring to impart sustained-release properties. The final dispersion contained both the free lidocaine (for rapid anesthetic effect) and the lidocaine encapsulated in nanoparticles (for prolonged effect). The prepared drug-polymer solution was carefully poured into silicone molds and sonicated for 1 hour to remove air bubbles and allow complete filling of the microneedle cavities. The filled molds were dried at room temperature for 36 hours. The prepared microneedle patches were stored for further evaluation.

Zeta size and zeta potential analyses

The average particle size and zeta potential of the HPMC-based lidocaine nanoparticles were determined by using the Litesizer 500 (Anton Paar, Austria) dynamic light scattering (DLS) system. Lyophilized nanoparticle powder was redispersed in deionized water by vortexing and sonicated for 5 minutes. Any larger aggregates were avoided through filtration with a 0.22 µm syringe filter. The prepared nanoparticle suspension was then transferred to a polystyrene cuvette for storage at 25 °C. The backscatter angle was 175 to obtain the hydrodynamic diameter. In zeta potential measurement, the nanoparticle suspension was drawn into the folded capillary zeta cell. The electrophoretic mobility of nanoparticles was measured at 25 °C, while the zeta potential was calculated.

Optical evaluation of microneedle patches

The prepared FDMN patches were examined for visual and optical microscopy assessment to evaluate structural integrity and uniformity. For visual inspection, appropriate oblique and normal lighting was used to examine the patches for surface irregularities, air bubbles, cracks, or deformities. Uniformity in microneedle length, transparency and proper mold filling were also evaluated. High-resolution images were taken for documentation and comparison purposes. Further microscopic evaluation was performed with an optical microscope to analyze the microneedle morphology, sharpness of its tips and structural consistency. Angled images from different sides were taken to achieve a complete evaluation of microneedle formation. Any defects like fractures, irregularities at the base, or incomplete needle formation were observed.

Scanning electron microscopy

Scanning electron microscopy (SEM) (Zeiss, Germany) was utilized for the evaluation of surface morphology and structural characteristics of prepared FDMNs patches and HPMC-based lidocaine nanoparticles. For imaging, FDMN patches have been mounted on aluminum stubs using double-sided conductive carbon tape with the microneedles oriented upright. Lyophilized nanoparticles were also spread on a stub evenly for clear structural details. SEM imaging was done at an accelerating voltage of 5-20 kV under various magnifications for measurement of microneedle shape, sharpness of tips and uniformity. On the other hand, SEM analysis offered particle-specific information about their dimensions, shapes, and surface textures.

Fourier transform infrared spectroscopy

Fourier transform infrared (FTIR) spectroscopy was employed to analyze the interactions and functional groups present in the HPMC-based lidocaine nanoparticles loaded microneedle patch (FDMN6). Spectral analysis was performed with an FTIR spectrophotometer (Alpha II, Bruker) in the range 4000–400 cm^{-1}. Samples including pure lidocaine, HPMC, PVP, HA and the final FDMN patch were analyzed to detect potential interactions between the drug and polymers.

Drug loading efficiency

The loading efficiency (LE) and encapsulation efficiency (EE) of lidocaine into HPMC nanoparticles were determined using an indirect method of quantification. An amount of 10 mg of lyophilized nanoparticles was dispersed in 10 mL of deionized water, and the dispersion was centrifuged for 30 minutes at 4 °C at 12,000 rpm to separate any unencapsulated drug. Free lidocaine from the centrifuged supernatant was quantified using UV-visible spectrophotometry (U2001, Hitachi, Japan) at 262 nm. The drug concentration was determined by preparing a standard calibration curve of lidocaine in the same solvent. The percentages of drug encapsulation (EE%) and loading efficiency (LE%) were calculated using the equations given below (1):

$$EE\ (\%) = \frac{Total\ drug - Free\ Drug\ in\ Supernatent}{Total\ drug} \times 100$$

$$LE\ (\%) = \frac{Encapsulated\ drug}{Total\ weight\ of\ nanoparticles} \times 100 \qquad (2)$$

Uniformity of thickness

The uniformity of the thickness of the FDMN patches was tested using a Vernier caliper. Measurements were taken at different locations on each patch – center and edges – to assess any variation in thickness. Each measurement was repeated three times to confirm accuracy and reproducibility. To determine the thickness uniformity of the microneedle patches, calculations were made for average thickness and standard deviation (n = 3). A low standard deviation indicated consistent fabrication with assured mechanical integrity and drug delivery. The acquired data ensured an understanding of the precision of the microneedle-casting process and the formation of the polymeric film.[30]

Insertion of microneedles

The insertion ability of the prepared FDMN patch (FDMN6) was tested using Parafilm M® as a skin simulator model. It was folded into eight layers, each of

which was approximately 161 µm thick, to accommodate and simulate the mechanical properties of human skin. The layer was sequentially assigned to the remaining layers from Layer 1 (top) to Layer 8 (bottom) to evaluate the extent of microneedle penetration. The FDMN6 patch was placed on the surface of the folded Parafilm M and pressed with gentle thumb pressure for 30 seconds to facilitate microneedle insertion (n = 3). The patch was then peeled off and the Parafilm M layers were visually examined. High-resolution digital pictures were taken. The punch-holes on the Parafilm M were then studied under optical microscopy to remove any doubt about the perforations. The number of penetrated layers was assessed to clarify mechanical strength efficiency as well as the efficiency of microneedles.

Ex-vivo *release study*

Ex-vivo release study has been conducted to evaluate and compare the release of different formulations, which included Lignocaine gel (Howards) and the FDMN patch (FDMN6) having both free lidocaine and lidocaine nanoparticles in it. This study was performed with excised rat skin mounted on a Franz diffusion cell, which has an effective diffusion area of 1.0 cm^2 and a receptor compartment volume of 7.0 mL filled with phosphate-buffered saline (PBS, pH 7.4). The receptor medium was maintained at 37 ± 0.5 °C and stirred continuously at 300 rpm to ensure proper mixing and sink conditions. Excised rat skin was wiped with ethanol to remove any adhering fat before placing it tightly between the donor and receptor compartments, stratum corneum facing the donor chamber. Each formulation was applied topically: Lignocaine 2% gel was spread evenly, a dual-approach FDMN patch was applied with gentle pressure to ensure proper adhesion and then hydrated with a few drops of PBS to initiate dissolution. 0.5 mL of sample was withdrawn from the receptor medium at predetermined time intervals, *i.e*., 0, 5, 15, 30, 60, 120, 180, 240, 360 and 480 minutes, with an immediate replacement of an equal volume of PBS to maintain sink conditions (n = 3). The collected samples were analyzed for concentration of lidocaine using a UV-visible spectrophotometer U2001, Hitachi, Japan (λ_{max} ~262 nm). The percentage cumulative drug release was determined as a function of time for each formulation and kinetic modeling was applied to determine the best fitting model. The release profiles were compared to evaluate whether the dual-approach FDMN patch has superior release through the obtainment of rapid lidocaine absorption from the free drug component, while ensuring sustained release from the lidocaine nanoparticles.

Biocompatibility testing (skin irritation study)

A skin irritation study was performed to confirm the biocompatibility of the developed FDMN patch (FDMN6) by using the Draize scoring method. All animals experiments were performed after receiving approval from the Animal Ethical Committee vide letter No. RIU/RIPS-RC/24/009A dated April 15, 2024. Healthy rats (n = 3) were chosen for the experiment, and the dorsal region was prepared carefully without cuts and abrasions by removing their hair with EU® hair removal cream. Rats were sorted into two groups: one group was treated with an FDMN patch placed on the dorsal skin using gentle pressure with the thumb and the second group served as a control. After 6 hours of application, the FDMN patch was carefully removed and the rats were observed for indications of irritation, like erythema, edema, and other visible skin reactions. The Draize scoring system grades such irritation according to the severity of the skin reactions. The skin was further monitored for 24 hours to view any delayed response concerning irritation. The collected scores were analyzed statistically to determine if the FDMN patch caused any significant irritation when compared with the control ones. Thus, the study has been conducted to ascertain the biocompatibility of the developed microneedle patch for safe transdermal applications.

In-vivo *evaluation of anesthetic effects*

In-vivo evaluation of the anesthetic effect produced by a prepared FDMN patch (FDMN6) was assessed and compared with that of a marketed lidocaine gel (Lignocaine 2%, Howards) in healthy rats (n = 3). Rats were divided randomly into 3 groups. Group 1 served as the control. Rats in Group 2 were treated with Lignocaine 2% gel, and Group 3 was treated with the prepared lidocaine nanoparticle loaded MN patch. For proper application of formulations, the dorsal skin of all the rats was cleared of hair with EU® hair removal cream exactly 24 h before the experiment. Each formulation was applied carefully to ensure uniform contact over a defined area (~1 cm^2) on the dorsal skin of the rat. The control group was also left untreated for baseline purposes to evaluate the pain sensitivity. An evaluation of the anesthetic effect was conducted using a mechanical nociception test. A standardized syringe needle pinch test was performed by applying pressure to the treated skin area and recording the intensity of response (flinch, vocalization, or withdrawal reaction).[31] The timing of the response latency was recorded at several time points (5, 15, 30, 60, 120, 240, 480 minutes post-application) to determine the onset and duration of anesthesia. Statistical analysis was conducted in order to compare the duration of anesthesia in groups treated with the respective formulation with the respective controls used as reference for the normal pain sensitivity.

Statistical analysis

All experimental data were processed and analyzed through the application of proper statistical tools. The results of *ex-vivo* release studies were analyzed statistically with the assistance of GraphPad Prism 8, using one-way ANOVA, followed by post-hoc analysis

to compare the differences between formulations. The data obtained from FTIR were analyzed by using Origin software. Mean values and standard deviations (mean ± SD) were calculated for all quantitative studies, including microneedle thickness uniformity and drug loading efficiency, using Microsoft Excel. A p-value of <0.05 was interpreted as statistically significant for all comparisons (n = 3). Data were expressed as mean ± SD and plotted graphically.

RESULTS AND DISCUSSION

Preparation of nanoparticle loaded fast-dissolving microneedle patches

The development of nanoparticle-loaded fast-dissolving microneedle (FDMN) patches commenced with making the chitosan nanoparticles loaded with lidocaine initially meant for incorporation in an HA-PVP-based microneedle matrix. However, during the formulation stage, the incorporation of chitosan nanoparticles into the HA-PVP solution caused an immediate drop in viscosity and visible precipitation. This observation suggested possible physicochemical incompatibilities or ionic interactions between the anionic charges inherent in HA and the cationic feature of chitosan, which might have caused instability in the colloidal system, resulting in a non-uniform formulation. As a remedy, HPMC was used as a different polymer for preparing the nanoparticles. The HPMC-based lidocaine nanoparticles had excellent compatibility with the HA-PVP microneedle matrix, resulting in a formulation that was stable and homogenous without precipitation. Based on physical characteristics, uniform drug distribution and ease of mold casting, FDMN6 was considered as optimum among the formulations prepared. This formulation was selected as the best patch for subsequent characterization due to its superior structural integrity and handling properties.

Zeta size and zeta potential analyses

Dynamic light scattering DLS (Litesizer 500, Anton Paar, Austria) was used to measure the particle size distribution and surface charge of HPMC-based lidocaine nanoparticles. The measured value of the average particle diameter (Z-average) was 71.40 ± 2.28 nm (Fig.1(a)), indicating that the particles were formed in the nanoscale range, which should enhance skin permeation through microneedles. The polydispersity index (PDI) was found to be 0.312, signifying that the size distribution is moderately narrow and acceptable, and the suspension is stable.

Zeta potential revealed a surface charge of -0.1 mV, which confirmed that the nanoparticles were almost neutral in charge (Fig. 1 (b)).

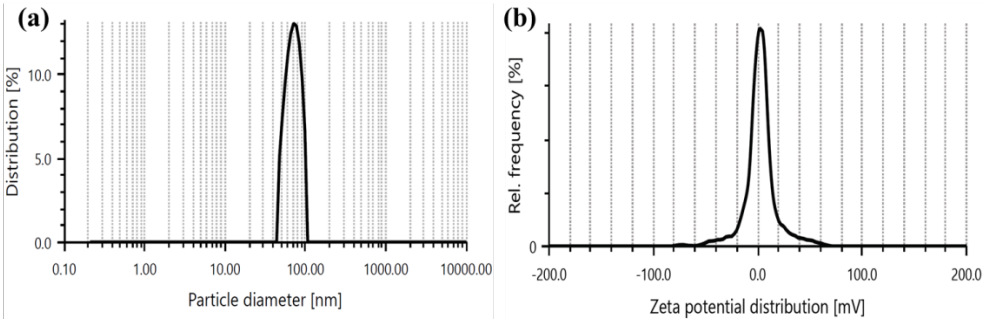

Figure 1: Size distribution and surface charge of prepared microneedle patch (FDMN6)

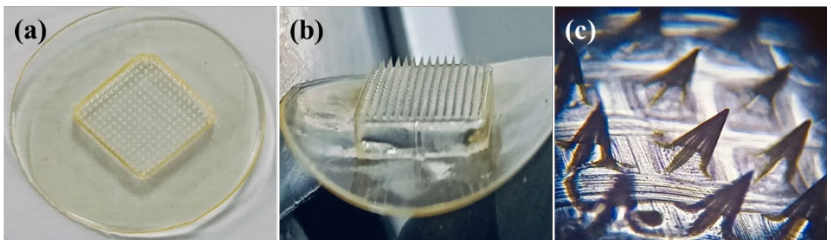

Figure 2: Morphological evaluation of FDMN6: a) arial view, b) side view and c) microscopic view

Although a highly negative or positive zeta potential (>±30 mV) is desirable for long-term physical stability of nanoparticle suspension, here, steric stabilization by HPMC (a neutral sterically stabilizing polymer) was presumed to give enough stabilization due to steric hindrance rather than

electrostatic repulsion. Owing to steric stabilization, no aggregation was observed, nor was any instability encountered during the formulation and handling, indicating that the system remained physically stable under the experimental conditions, despite a lower zeta potential. These results support the suitability of HPMC-based nanoparticles for incorporation into the microneedle matrix for sustained lidocaine delivery. Additionally, there was no aggregation of nanoparticles upon storage over four weeks at 4 °C, which confirmed their long-term stability.

Optical evaluation of microneedle patch

The prepared FDMN6 patch was evaluated visually and microscopically to assess its physical integrity, microneedle morphology, and fabrication uniformity. The microneedle patch has a transparent and flexible backing layer, with the microneedle arrays uniformly distributed across the entire surface, making it visible even to the naked eye (Fig. 2 (a)). The visual inspection showed excellent structural integrity through the absence of air bubbles, cracks, or deformations. Figure 2 (b) depicts the three-dimensional architecture of microneedles filling the mold cavities completely and forming well-defined needle structures with conical geometry. Under optical microscopy (Fig. 2 (c)), the sharp-pointed microneedles showed uniform alignment, very important for skin penetration. There were no structural imperfections like tip bending, fractures, or incomplete formation, indicative of the polymeric formulation having adequate viscosity and strength to replicate the mold pattern quite precisely. The visual and microscopic observations offered a confluence of evidence pointing to the high-quality and reproducibility of the fabrication process for FDMN6 patches.

Scanning electron microscopy

Scanning electron microscopy (SEM) was employed to investigate lidocaine-loaded nanoparticles and microneedle (MN) patch surface morphology and structural characteristics, as shown in Figure 3. SEM photomicrographs of nanoparticles were shown in Figure 3 (a-c) at different magnifications, *i.e*., 5,000X, 10,000X, and 15,000X. The nanoparticles possessed a nearly spherical shape, with a smooth surface and uniform distribution, confirming successful formulation with minimum aggregation. From the SEM observations, the estimated particle sizes were in the nanometric range, corresponding well to the expected range of size for efficient dermal delivery.

Figure 3 (d-f) illustrates the microneedle patch at 54X, 100X, and 175X magnifications. The microneedles were arranged in a regular array and exhibited consistent conical geometry and sharp tips for effective skin penetration. The average microneedle height was confirmed to be around 500 µm, with the base width approximately 200 µm. At the highest magnification, the radius of the sharp tip (Fig. 3 (f)) was visible and appeared to be under 20 µm, which is sufficient for forming micropores, without causing significant pain. In addition, the microneedle surface showed nanoparticulate material binding in confirmation of effective lidocaine nanoparticle inclusion or surface loading. Such deposition could be contributing to rapid dissolution, as well as enhanced local availability of the drug following skin insertion. The combined morphological properties confirm that the prepared microneedle patch is mechanically stable and efficient in transdermal delivery of the nano-sized drug payload. Efficient surface area and permeation are provided by the nanoscale particle size, while the painless administration as well as stable delivery of the drug are provided by the mechanical microneedle structure.

Table 2
Quantitative comparison of key physical characteristics of FDMN6

Parameter	Mean ± SD
Microneedle height (µm)	500 ± 10
Base width (µm)	200 ± 5
Insertion depth (µm)	483 ± 8
Particle size (nm)	71.4 ± 2.28
PDI	0.312 ± 0.01
Zeta potential (mV)	-0.1 ± 0.02
Drug loading efficiency (%)	8.5 ± 0.65
Entrapment efficiency (%)	94.5 ± 1.93

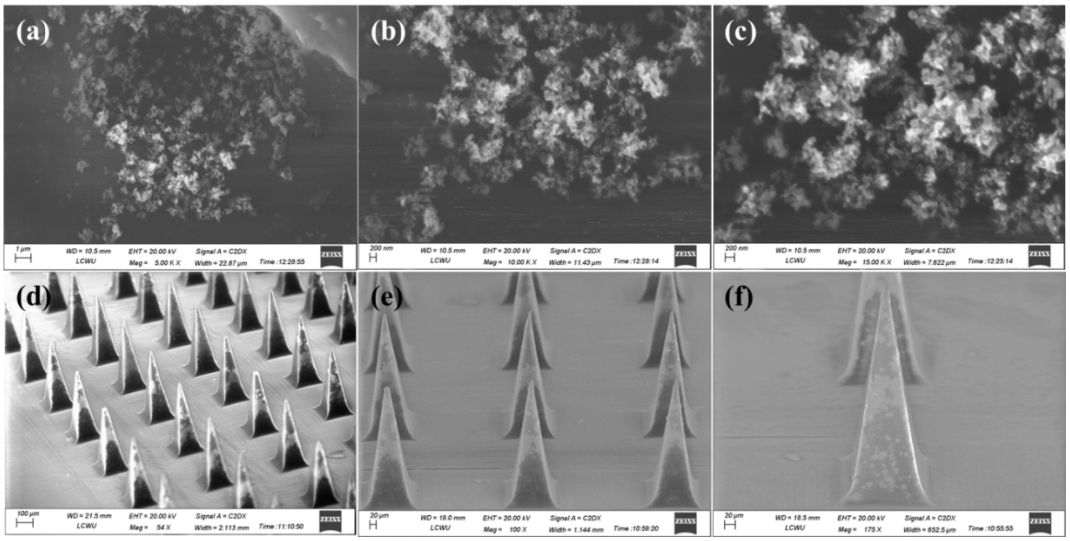

Figure 3: SEM images of prepared nanoparticles and FDMN6 patch

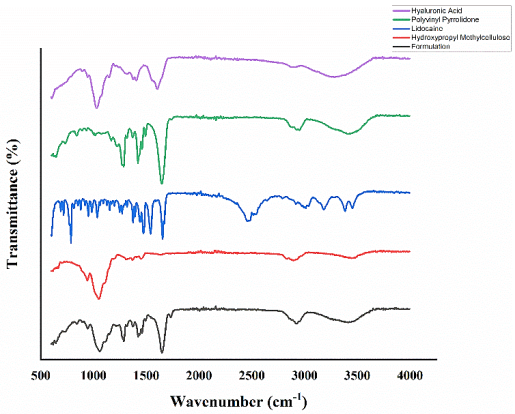

Figure 4: FTIR spectra of individual ingredients and prepared FDMN6 patch

Such findings provide excellent proof for the efficacy of the formulation as a useful platform for transdermal delivery of lidocaine. A quantitative comparison of key physical characteristics of FDMN6 is shown in Table 2.

Fourier transform infrared spectroscopy

The obtained spectra of each component were checked to confirm chemical integrity and suggest possible interactions (Fig. 5), including HA, PVP, lidocaine, HPMC, and finally the mixture. The spectrum of HA showed peaks at ~3200–3400 cm^{-1} for O–H and N–H stretching, 1600–1650 cm^{-1} for amide I and C=O stretching, and 1400 cm^{-1} for symmetric stretching by carboxylate groups. These peaks match the polysaccharide nature and hydrophilicity of HA. The main absorbance peaks for PVP were noted at around 1650 cm^{-1} corresponding to C=O stretching of the pyrrolidone ring and 1280 cm^{-1} corresponding to C-N stretching of the polymer. There was also a broad band around 2900 cm^{-1} due to C-H stretching.

The drug showed absorptions at ~3300 cm^{-1} for N-H amide stretching, 1640 cm^{-1} for C=O amide stretching, and 1270 cm^{-1} for C-N stretching, consistent with its aromatic and amide functional groups. HPMC distinctly showed its backbone of cellulose with peaks at 3400 cm^{-1} (O-H stretching), 2900 cm^{-1} (C-H stretching), and 1050 cm^{-1} (C-O-C ether linkage). The FTIR spectrum of the final formulation retained the prominent peaks of all the ingredients without significant shifts or loss of functional groups, suggesting no covalent interaction between lidocaine and excipients. The O–H/N–H stretching region (3200–3400 cm^{-1}) showed broadening due to overlapping contributions from HA, HPMC, and PVP. The amide I band (1640–1650 cm^{-1}) was preserved, showing structural integrity of lidocaine. No new peaks were observed, ruling out chemical degradation or complexation.

Thus, the FTIR findings confirmed the compatibility of lidocaine with the selected polymers (HA, PVP, HPMC) within the microneedle system. The absence of any antagonistic interactions recommends the use of this system in drug delivery.

Drug loading efficiency

Entrapment efficiency (%) and drug loading efficiency (%) of lidocaine within the HPMC-based nanoparticles incorporated in the FDMN6 microneedle patch were analyzed to investigate the formulation capability to deliver and sustain the active pharmaceutical ingredient. The results indicated high entrapment efficiency (EE%) of 94.5 ± 1.93% and a drug loading efficiency (LE%) of 8.5 ± 0.65%. This indicates that the lidocaine added in the process of nanoparticle synthesis was entrapped effectively in the polymeric matrix with minimal loss of the drug.

Uniformity of thickness

The thickness should be consistent at the base of the microneedle patch to ensure patch strength. The thickness of the prepared patch (FDMN6) was measured with a Vernier caliper at various points on the edges of each patch. It was found to be on average 0.173 ± 0.01mm, with negligible variation in thickness over different parts of the patch. Such thickness uniformity indicates a highly reproducible casting of the polymeric solution during patch preparation, thereby making sure that each microneedle patch will provide an equivalent strength and have consistent mechanical properties. Besides being critical for insertion depth determination, patient safety demands uniform thickness to define a predictable dissolution rate. The very low deviation from the mean supports the strength of the patch, thus depicting an optimized formulation.

Insertion of microneedles

The insertion capability of the FDMN6 patch was evaluated using Parafilm M® skin simulant, folded in eight layers (~161 µm per layer) to mimic the mechanical resistance of human skin. The microneedle patch was gently pressed with a thumb for 30 seconds (Fig. 5 (a)), and the layers were inspected visually and microscopically to determine the depth of microneedle insertion. Microscopic analysis revealed that the microneedles penetrated well into the third layer, corresponding to an insertion depth of around 483 µm, as shown in Figure 5 (b-d). In the fourth layer, there were no holes observed, as shown in Figure 5 (e). The apparent occurrence of perforation in the outermost three layers confirmed the mechanical strength and structural sharpness of the microneedles, enabling them to penetrate efficiently upon manual pressure. These results indicate that the FDMN6 patch has a sufficient insertional capacity to penetrate the stratum corneum, so that the drug can be delivered across the skin. The depth of penetration is considered suitable for intradermal delivery of lidocaine and supports the envisioned dual-release anesthetic effect.

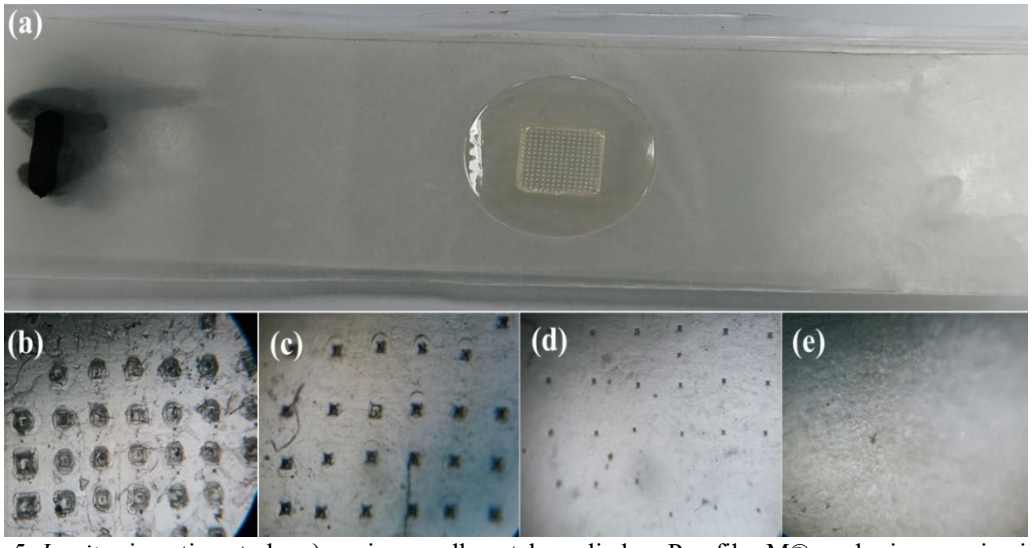

Figure 5: *In-vitro* insertion study: a) a microneedle patch applied on Parafilm M®, and microscopic views of b) first layer, c) second layer, d) third layer and e) fourth layer

***Ex-vivo* release study**

The *ex-vivo* release study was performed to characterize lidocaine release from the optimized dual-action FDMN patch, as compared to a marketed lidocaine gel (2%). There was a gradual sustained release pattern of lidocaine from the FDMN6 patch, with a mean percentage cumulative release of 92.87 ± 0.88% over 480 minutes of study, whereas the marketed gel showed a faster release initially, with release percentages of 45.96±3.397% in 120 minutes and 47.11 ± 0.722% at 240 minutes (Fig. 6 (a)), signifying a very short release behavior, with very little extension with time. These results revealed that a dual drug delivery system achieved by the FDMN6 patch was able to couple the immediate release of free lidocaine with the sustained release of HPMC-based lidocaine nanoparticles, thus establishing an extended delivery period required to prolong the anesthetic action. The better release of FDMN6 is attributed to the dual delivery approach, control of the polymeric matrix, and efficient penetration of the skin via microneedles. In Figure 6 (b), the schematic illustration of the release mechanism is shown.

The release data were fitted to various kinetic models to understand the release mechanism (Table 3). For FDMN6, the best fit was found for the first-order kinetic model (R^2 = 0.983), suggesting concentration-dependent drug release, which is typically associated with diffusion and erosion-controlled systems. The Korsmeyer-Peppas model also yielded a high coefficient of determination (R^2 = 0.975, n = 0.185), suggesting a Fickian diffusion-based release pathway as the major release avenue. The Higuchi model (R^2 = 0.864) supported this result by confirming diffusion-controlled release from a porous matrix. The marketed gel followed Higuchi kinetics (R^2 = 0.967) and had a Korsmeyer-Peppas n value of 0.400, which signifies anomalous (non-Fickian) transport, almost certainly a consequence of the semi-solid matrix of the gel. Overall, these findings prove that the FDMN6 microneedle patch demonstrates a dual-phase, diffusion-controlled release, with better patient compliance and longer-lasting anesthetic time, compared with the conventional topical formulation.

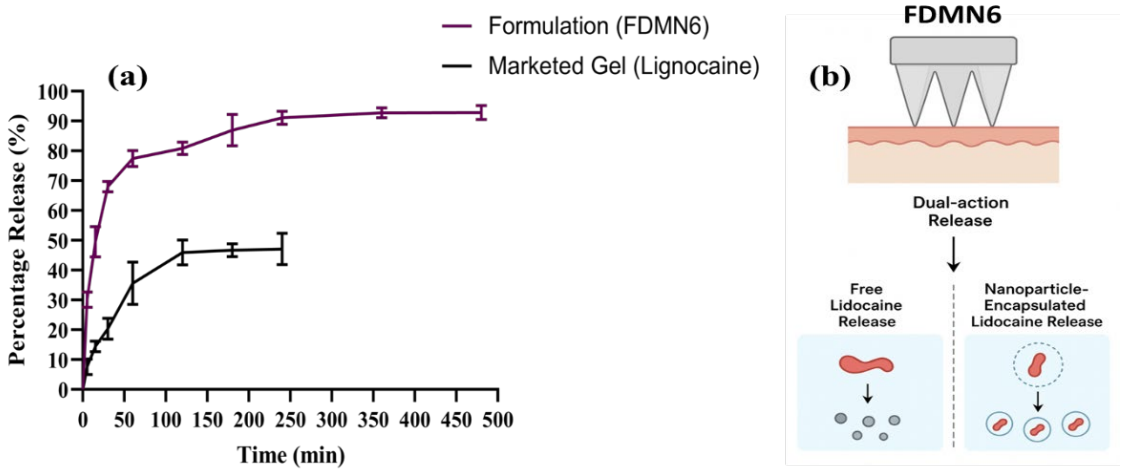

Figure 6: a) Comparison between *ex-vivo* release of a commercial gel and FDMN6; and b) schematic illustration of the dual-action release mechanism

Biocompatibility testing (irritation study)

The Draize scoring method was used to evaluate the biocompatibility of the FDMN6 patch for transdermal application on healthy rats. The hair was removed (Fig. 5 (a)) and a patch was applied to the shaved dorsal area of the rats for 6 hours (Fig. 7 (b)), while another group served as an untreated control and did not receive any treatment. After the removal of the patch, the skin was assessed for different signs of irritation, including erythema, edema, or any other visible inflammatory response (Fig. 7 (c)). There were no evident signs of irritation, redness, or swelling on the application site upon immediate post-removal observation and 24 hours after patching. The Draize score for the treated group remained '0' at all times during the observation, thus asserting lack of acute dermal reactions. The effort was comparatively paralleled by the control group, which did not show any sign of irritation either.

Table 3
Kinetic models

FDMN6										Commercial gel									
Zero order		First order		Higuchi		Korsmeyer-Peppas		Hixson-Crowell		Zero order		First order		Higuchi		Korsmeyer-Peppas		Hixson-Crowell	
R^2	K0	R^2	k1	R^2	kH	R^2	n	R^2	kHC	R^2	k0	R^2	k1	R^2	kH	R^2	n	R^2	kHC
0.708	0.283	0.983	0.038	0.864	5.699	0.975	0.185	0.884	0.003	0.881	0.259	0.928	0.004	0.967	3.570	0.975	0.400	0.913	0.001

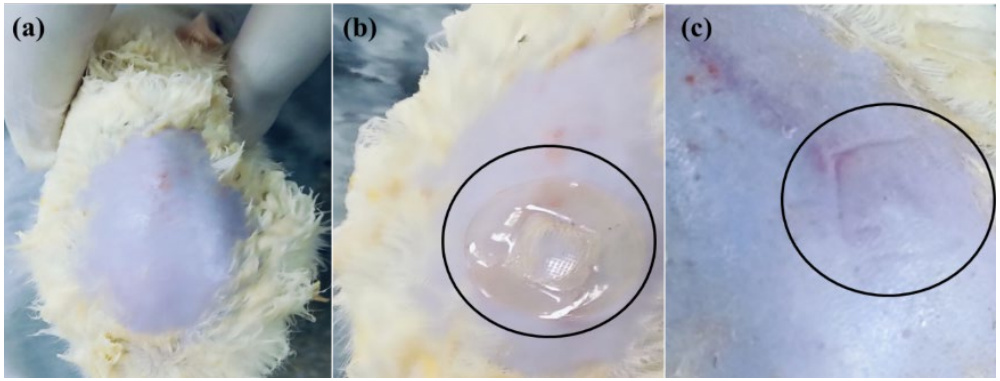

Figure 7: Biocompatibility study of FDMN6, a) before application, b) with the patch and c) after patch application

These findings confirm the high biocompatibility of the FDMN6 patch. The presence of biocompatible polymers, such as HPMC, PVP, and HA, in the formulation and the microneedles being non-invasive and dissolvable confirmed well skin tolerability.

***In-vivo* evaluation of anesthetic effects**

The *in-vivo* anesthetic efficacy of the prepared dual-approach FDMN6 patch was compared with a commercial lidocaine gel (Lignocaine 2%) and an untreated control. The experiment was conducted on rats (n = 3 per group), and to each of them a treatment preparation was applied on the shaved dorsal skin. The anesthetic effect was evaluated by a mechanical nociception test, with a standardized needle pinch being administered at standardized time intervals and response latency (flinch, vocalization, or withdrawal) being observed. In the control group (Group 1), immediate and constant pain reactions were observed throughout the study, confirming normal sensitivity to pain. Group 2, which received the Lignocaine gel, experienced a rapid onset of anesthesia, with latency of response increasing in the first 5 minutes. The effect was short-lived, however, as a return to the baseline pain response occurred after 60–90 minutes, indicating minimal duration of action (Fig. 8 (a-d)).

On the other hand, the FDMN6 group (Group 3) showed both early and prolonged anesthetic durations. There was a visible effect of anesthesia in the first 5–15 minutes caused by the free lidocaine in the patch. More importantly, the effect lasted up to 480 minutes, which is significantly longer than in the case of the gel group (Fig. 8 (e-i)). Quantitative reaction latency time showed significantly prolonged response times in the FDMN6 group up to 480 minutes ($p < 0.05$), whereas the group with the Lignocaine gel returned to baseline levels by 60–90 minutes (Table 4). This description of extended duration is due to the sustained release of lidocaine from the HPMC-based nanoparticles incorporated into the microneedle matrix.

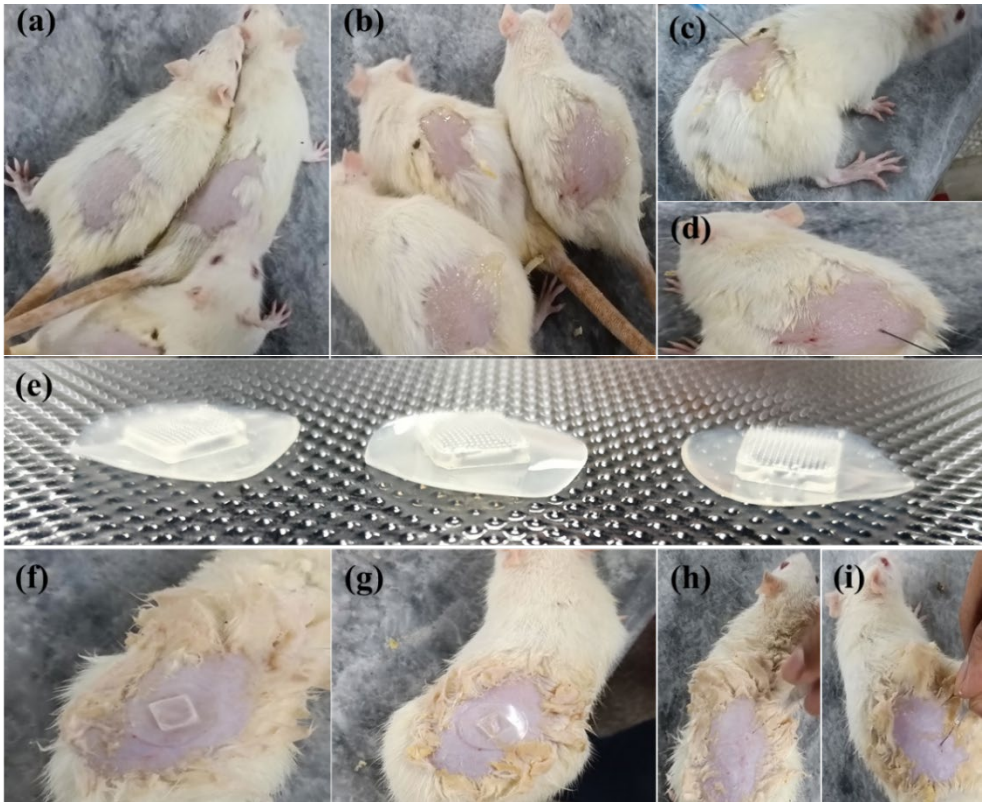

Figure 8: *In-vivo* evaluation of anesthetic effects: a) without application of Lignocaine gel, b) after application of Lignocaine gel, c-d) evaluation of response to a needle pinch, e) microneedle patches, f-g) application of microneedle patches and h-i) evaluation of response to a needle pinch after the application of the microneedle patch

Table 4
Reaction latency time

Time (min)	Group 1 Control	Group 2 Lidocaine gel	Group 3 FDMN6 patch
0	0.3 ± 0.1 s	0.3 ± 0.1 s	0.3 ± 0.1 s
5	0.3 ± 0.1 s	1.2 ± 0.2 s	1.4 ± 0.2 s
15	0.3 ± 0.1 s	1.0 ± 0.1 s	1.8 ± 0.3 s
30	0.3 ± 0.1 s	0.6 ± 0.1 s	1.7 ± 0.2 s
60	0.3 ± 0.1 s	0.4 ± 0.1 s	1.5 ± 0.2 s
120	0.3 ± 0.1 s	0.3 ± 0.1 s	1.3 ± 0.2 s
240	0.3 ± 0.1 s	0.3 ± 0.1 s	0.9 ± 0.1 s
480	0.3 ± 0.1 s	0.3 ± 0.1 s	0.6 ± 0.1 s

These results confirmed the superior *in-vivo* performance of the prepared dual-action FDMN6 patch. The obtained data support the therapeutic potential of this system for clinical applications requiring a long-lasting local anesthesia effect.

CONCLUSION

A novel dual-action fast-dissolving microneedle (FDMN) patch was developed in this study for the localized delivery of lidocaine with the objective of overcoming shortcomings posed by conventional topical and injectable anesthetics. The formulation incorporated both free lidocaine for rapid onset and HPMC-based lidocaine nanoparticles for sustained release. The prepared patch (FDMN6) was characterized by physical integrity, uniform microneedle morphology, high drug entrapment efficiency, and good skin insertion capability. *Ex-vivo* studies indicated that the release of lidocaine from the novel patch was significantly enhanced and prolonged when compared with a commercial lidocaine gel. The patch exhibited excellent biocompatibility, with no irritancy observed in the animal models. The *in-vivo* assessment also showed that the FDMN6 patch was effective in providing rapid and prolonged anesthesia that was sustained over a longer period of time, compared to the conventional gel formulation. Future work may focus on clinical translation and exploring its potential for other short-acting therapeutic agents. The developed FDMN6 patch can be optimized for human application by focusing on large-scale reproducibility and controlled drug loading uniformity.

REFERENCES

[1] C. N. Giordano, L. Gill, E. M. Feldman and A. W. James, *Curr. Dermatol. Rep.*, **4**, 97 (2015), https://doi.org/10.1007/s13671-015-0110-9

[2] G. Paladini, M. Tedesco, G. Carabelli and G. Petroni, *J. Pain Res.*, **13**, 285 (2020), https://doi.org/10.2147/JPR.S211234

[3] M. Daryab, M. Hasani, R. Rashid and N. Moghaddam, *Iran. J. Pharm. Res.*, **21**, e123787 (2022), https://doi.org/10.5812/ijpr.123787

[4] J. Gudin and S. Nalamachu, *Postgrad. Med.*, **132**, 28 (2020), https://doi.org/10.1080/00325481.2019.1702296

[5] F. Qu, C. Gu, J. Zhang and Y. Ma, *Theranostics*, **12**, 3372 (2022), https://doi.org/10.7150/thno.69999

[6] R. Ijaz, S. Ali, M. Ahmed and Z. Altaf, *BioNanoScience*, **14**, 1397 (2024), https://doi.org/10.1007/s12668-024-01428-7

[7] S. Ali, Z. Altaf, R. Ijaz and Z. Ahmad, *BioNanoScience*, **15**, 181 (2025), https://doi.org/10.1007/s12668-025-01799-5

[8] Z. Altaf, S. Ali, A. Shahid and Z. Ahmad, *Inflammopharmacology*, **33**, 1381 (2025), https://doi.org/10.1007/s10787-025-01696-z

[9] T.-M. Don, Y.-C. Chen, C.-Y. Lin and W.-C. Chen, *Int. J. Biol. Macromol.*, **207**, 90 (2022), https://doi.org/10.1016/j.ijbiomac.2022.02.127

[10] M. A. Luzuriaga, M. L. Berry and R. S. Bartlett, *Lab Chip*, **18**, 1223 (2018), https://doi.org/10.1039/C8LC00098K

[11] M.-C. Chen, M.-H. Ling, K.-Y. Lai and E. Pramudityo, *Biomacromolecules*, **13**, 4022 (2012), https://doi.org/10.1021/bm301293d

[12] B. Chanabodeechalermrung, W. Phitak, T. Sritapunya and N. Meepowpan, *Polymers*, **16**, 452 (2024), https://doi.org/10.3390/polym16040452

[13] M. Jin, L. Zhang, X. Yang and C. Zhao, *Drug Deliv. Transl. Res.*, **12**, 415 (2022), https://doi.org/10.1007/s13346-021-01046-w

[14] J. Chudzińska, A. Wawrzyńczak and A. Feliczak-Guzik, *Polymers*, **16**, 1396 (2024), https://doi.org/10.3390/polym16101396

[15] I. Saha and V. K. Rai, *Carbohyd. Polym.*, **267**, 118168 (2021), https://doi.org/10.1016/j.carbpol.2021.118168

[16] X. Li, W. Wang, J. Zhao and H. Liu, *Int. J. Biol. Macromol.*, **282**, 137185 (2024), https://doi.org/10.1016/j.ijbiomac.2024.137185

[17] Y. Luo, Z. Wang and T. Sun, *AAPS PharmSciTech*, **22**, 1 (2021), https://doi.org/10.1208/s12249-020-01909-4
[18] H. Alzain, A. Bakr, F. Elsheikh and M. Al-Ghamdi, *Green Process. Synth.*, **12**, 20230011 (2023), https://doi.org/10.1515/gps-2023-0011
[19] M. Abd El-Kader, N. El-Kady and R. Hegazy, *J. Mater. Res. Technol.*, **13**, 291 (2021), https://doi.org/10.1016/j.jmrt.2021.04.055
[20] W. Han, S. Zhang and L. Xu, *Small*, **19**, 2301670 (2023), https://doi.org/10.1002/smll.202301670
[21] S. Noreen, R. Aslam and T. Hussain, *Drug Deliv. Transl. Res.*, **12**, 2649 (2022), https://doi.org/10.1007/s13346-022-01152-3
[22] W. Y. Jeong, S. H. Yoon and Y. Park, *Biomater. Res.*, **25**, 1 (2021), https://doi.org/10.1186/s40824-021-00226-6
[23] A. Zarepour, A. Soozanipour and A. Khosravi, *Curr. Opin. Biomed. Eng.*, **35**, 100602 (2025), https://doi.org/10.1016/j.cobme.2025.100602
[24] A. Javed, S. Rehman, H. Jameel, Z. Ahmad and A. Yousaf, *Naunyn-Schmiedeberg's Arch. Pharmacol.*, **398**, 6739 (2025), https://doi.org/10.1007/s00210-024-03708-1
[25] A. Yousaf, Z. Ahmad, H. Jameel, S. Rehman and A. Javed, *J. Pharm. Innov.*, **20**, 104 (2025), https://doi.org/10.1007/s12247-025-10007-6
[26] P. Pan, H. Chen, L. Sun and Y. Liu, *Pharmaceutics*, **15**, 2360 (2023), https://doi.org/10.3390/pharmaceutics15092360
[27] N. H. Hoang, T. D. Pham and H. T. Nguyen, *Polymers*, **14**, 662 (2022), https://doi.org/10.3390/polym14040662
[28] N. Van Bavel, A. Jacobs and F. Verheyen, *Molecules*, **28**), 4328 (2023), https://doi.org/10.3390/molecules28114328
[29] E. Azizoglu, O. Ozer and M. R. Prausnitz, *Drug Deliv. Transl. Res.*, **12**, 444 (2022), https://doi.org/10.1007/s13346-021-01047-9
[30] P. W. R. Ananda, R. Jayasinghe and C. Wickramarachchi, *Int. J. Pharm.*, **609**, 121204 (2021), https://doi.org/10.1016/j.ijpharm.2021.121204
[31] N. Supachawaroj, K. Kerdmanee and S. Limsitthichaikoon, *Gels*, **10**, 739 (2024), https://doi.org/10.3390/gels10110739